Disruptive and protective outcomes to memory and attention when treating diffuse glioma

Romero-Garcia R[1,*,§], Suckling J[1,2,3,*], Owen M[1], Assem M[4], Sinha R[5], Coelho P[6], Woodberry E[7], Price SJ[5], Burke GAA[8], Santarius T[5,9], Erez Y[4], Hart MG[5]

* These authors contributed equally

1. Department of Psychiatry, University of Cambridge; 2. Behavioural and Clinical Neuroscience Institute, University of Cambridge; 3. Cambridge and Peterborough NHS Foundation Trust; 4. MRC Cognition and Brain Sciences Unit, University of Cambridge; 5. Department of Neurosurgery, Addenbrooke's Hospital, Cambridge; 6. Neurophys Limited; 7. Department of Neuropsychology, Cambridge University Hospitals NHS Foundation Trust, 8. Department of Paediatric Haematology, Oncology and Palliative Care, Addenbrooke's hospital, Cambridge; 9. Physiology, Development and Neuroscience, University of Cambridge,

§ Correspondence to: Rafael Romero-Garcia PhD, University of Cambridge, Department of Psychiatry, Herchel Smith Building for Brain and Mind Sciences, Robinson Way, Cambridge CB2 0SZ, UK Email: rr480@cam.ac.uk

Keywords: Brain Tumours, structural MRI, diffusion MRI, Neurosurgery, Brain Networks, NODDI, Glioma, Cognitive function, memory, attention, patients

ABSTRACT

Surgical resection with adjuvant chemotherapy and radiotherapy are effective treatments to delay glioma progression and improve survival. Nevertheless, a large proportion of patients have treatment-induced cognitive deficits that dramatically reduce their life quality. Predicting the treatment-induced functional impairments is difficult due to the complex interlocking and diffusely spread networks that underpin different aspects of cognition. Here we investigated glioma interactions with brain networks in relation to cognitive recovery after surgical resection and during chemo-radiotherapy treatment. Seventeen patients with diffuse non-enhancing glioma (aged 22-56 years) were longitudinally MRI-scanned and cognitively assessed using a tablet-based screening tool before and after surgery, and during a 12-months recovery period. Using structural MRI and Neurite Orientation Dispersion and Density Imaging (NODDI) derived from diffusion-weighted images, we respectively estimated tumour overlap and Neurite Density (as an *in-vivo* proxy measure of axon and dendrite concentration) with brain networks and functional maps derived from normative data in healthy participants. We found that neither total lesion volume nor tumour location based on traditional lobular divisions were associated with memory or attention deficits. However, tumour and lesion overlap with the Default Mode Network (DMN), Attention Network and attention-related regions located in frontal and parietal cortex was associated with memory and attention deficits. This association was above and beyond the contributions of preoperative cognitive status and tumour volume (Linear Mixed Model, $P_{fdr}<0.05$). On the other hand, Neurite Density was reduced not only within the tumour, but also beyond the tumour boundary, revealing a distal effect with global consequences to brain networks. High preoperative Neurite Density outside the tumour, but within the Frontoparietal Network was associated with better memory and attention recovery. Moreover, postoperative and follow-up Neurite Density within the DMN, Frontoparietal and Attention Networks were associated with memory and attention improvements ($P_{fdr}<0.05$). We conclude that gliomas located on brain networks that are fundamental for cognitive processing mediate cognitive deficits and they exert a distal effect on Neurite Density in these networks that is also associated with cognitive recovery. Our work provides insights into the brain reorganisation that occurs due to the presence of a tumour and its subsequent removal, which has potential capability to predict cognitive outcomes. Understanding the pathophysiology underlying tumour related cognitive outcomes will be vital to the development of novel prognostic biomarkers, subgroup stratification in clinical trials, and individualised rehabilitation programmes.

INTRODUCTION

Every year more than 300,000 people worldwide face the diagnosis of a brain tumour. As a result of their tumours, a large proportion of patients develop cognitive deficits ranging from 29% in patients with non-irradiated low-grade glioma, to about 90% in patients following chemo-radiotherapy for metastases (Klein et al., 2002; Meyers et al., 2004). Patients who undergo surgical resection rather than biopsy have a better overall survival (Jakola et al., 2012), and extending the resection beyond the abnormality seen on MRI further improves prognosis (Yordanova et al., 2011). However, the extent of resection is only a worthwhile prognostic factor in the management of the tumour if subsequent cognitive functioning can be maintained, and therefore any impairment of brain structure and function is a significant risk factor for a reduction in quality of life (Santarius et al., 2019). Consequently, preoperative anticipation of post-surgical cognitive alterations represents a major interest for patients and clinicians alike.

Despite being recognised as a fundamental outcome measure of treatment success, cognitive deficits still remain one of the most unpredictable aspects of patients' prognosis (Taphoorn and Klein, 2004). Unfortunately, the impact of surgery on functional outcome has traditionally been underappreciated (Ferroli et al., 2015; Sagberg et al., 2017). Radiotherapy (Douw et al., 2009) and chemotherapy (Wefel and Schagen, 2012)(Douw et al., 2009)(Douw et al., 2009)(Douw et al., 2009) can also have a profound impact on several cognitive domains such as attention, executive functioning and information processing speed. Tumour- and treatment-induced cognitive impairment not only has a dramatic impact on patients' quality of life, but has also been recognised as a significant prognostic factor in patient survival (Klein et al., 2003).

Structural MRI provides important information about the brain and tumour and is currently the state-of-the-art imaging used in clinical practise for brain tumour diagnosis, planning of treatment and monitoring. However, typical MRI sequences used for clinical evaluation are limited by low biological specificity that limit their capability to differentiate tumour types and infiltration as well as determine macromolecular and histological compositions. For example, although gadolinium contrast enhancement is currently used with MRI as a marker of anaplastic transformation of diffuse lower-grade gliomas, up to one-third of high-grade gliomas are non-enhancing (Scott et al., 2002).

Recently developed MRI sequences that estimate tissue microstructure integrity have revolutionised *in-vivo* investigation of the human brain, but their applications to neuro-oncology have been limited. The capability of modern MRI protocols has been demonstrated for estimates of tumour infiltration (Li et al., 2018), grading (Fan et al., 2006), tumour heterogeneity (Just, 2014), tumour progression (Mohsen et al., 2013) and patient survival (Peng et al., 2013). The incorporation of recent MRI protocols into the clinical routine may be useful in reducing treatment-induced neurocognitive dysfunction in paediatric (Ajithkumar et al., 2017) and adult brain tumours (Ahles et al., 2012). Notwithstanding, most previous brain tumour studies have used tensor models to explore microstructural changes under the assumption of Gaussian diffusion processes. In contrast, the Neurite Orientation Dispersion and Density Imaging (NODDI) technique is a recently developed multi-shell sequence that uses varying gradients strengths to provide more specific measurements of tissue microstructure than traditional Diffusion Tensor Imaging (DTI) (Zhang et al., 2012). Intra-cellular diffusion estimation derived from NODDI as a marker of Neurite Density has been validated using histochemical analysis in mouse models (Wang et al., 2019) and has shown sensitivity to detect axonal degeneration in neurological conditions such as Alzheimer's (Colgan et al., 2016) and Parkinson's disease (Kamagata et al., 2016). Caverzasi *et al.* (2016) showed that even for tumour lesions that appear to be homogeneous on corresponding fluid-attenuated inversion-recovery (FLAIR) images, NODDI has the potential to differentiate infiltrative tumour components. Despite these promising findings, no study has yet used NODDI to evaluate the impact of tumours and their treatment on cognition.

Diffuse low-grade gliomas (DLGGs) are slow-growing and infiltrative tumours involving glial cells. The low proliferation rate restricts the "lesion momentum", which is defined broadly as the growth kinetics and the speed of a tumour's evolution, *i.e.* malignant progression. It has been suggested that the chronic and slowly progressive nature of these tumours allows more time for neuroplastic reorganisation which results in considerably more favourable survival rates compared to high-grade gliomas, but also has a protective effect on neurocognitive functioning (Wefel et al., 2016). Nevertheless, it is well established that although tumours and surgical resection represent focal lesions within the brain, tumours have an overall impact on cognitive performance (Anderson et al., 1990) and this may be mediated by a disruption of distant neuronal circuits. These "long-range" effects produced by focal brain tumour have been also observed at a functional level, with gliomas

reducing long-range functional connectivity (Harris et al., 2014; Maesawa et al., 2015; van Dellen et al., 2012) and globally disrupting functional integrity (Hart et al., 2019).

A major challenge when predicting the consequences of surgery and radio-chemotherapy is that higher-order cognitive functions are sub-served by communication across spatially extended neural circuits that cannot be completely captured using traditional localisation-based models and which, therefore, require whole-brain approaches. Large-scale brain networks represented by connectomics offer a holistic framework to analysing the brain as a circuit of interacting components by modelling brain regions as nodes and connections between regions as edges that are critically related to cognition (Bressler and Menon, 2010). In neuro-oncology, markers derived from brain network approaches have been demonstrated to be sensitive to the presence of low-grade gliomas (Xu et al., 2013), plasticity differences between low- and high-grade gliomas (van Dellen et al., 2012), and surgically induced alterations (Huang et al., 2014). Consequently, the use of brain network data to explore the potential for cognitive disruption induced by brain tumours and their treatment could be of major clinical relevance.

In this longitudinal study, we prospectively investigated whether the interaction between tumours and normative brain networks derived from healthy participants can predict cognitive recovery postoperatively and during a follow-up period of 12 months. We hypothesised that surgically-induced cognitive deficits are associated with disruption of brain networks that have been previously identified as fundamental for cognition.

METHODS

Sample

This study is a single centre prospective cohort design approved by the Cambridge Central Research Ethics Committee (protocol number 16/EE/0151). Patients were identified at adult neuro-oncology multidisciplinary team (MDT) meetings at Addenbrooke's Hospital (Cambridge, UK), and a consultant neurosurgeon directly involved in the study identified potential patients based on the outcome of the MDT discussion. Inclusion criteria included: (*i*) Participant is willing and able to give informed consent for participation in the study, (*ii*) imaging is evaluated by the MDT and judged to have typical appearances of a glioma, (*iii*) Stealth MRI is obtained (routine neuronavigation MRI scan performed prior to surgery), (*iv*) WHO performance status 0 or 1 (Hunter, 1980), (*v)* 18 ≤ Age ≤ 80, (*vi*) tumour located in or near eloquent areas of the brain thought to be important for speech and executive functions, and (*vii*) patient undergoing awake surgical resection of a diffuse glioma. This last inclusion criterion was adopted to collect additional intraoperative electrocorticography data that will be reported elsewhere. Participants were excluded if any of the following applied: *i*) concomitant anti-cancer therapy (except for dexamethasone treatment), (*ii*) history of previous malignancy (except for adequately treated basal and squamous cell carcinoma or carcinoma in-situ of the skin) within 5 years, and (*iii*) previous severe head injury.

We recruited 17 patients aged 22-56 years (8 females) with different grades of glioma: WHO-I N=2, WHO-II N=7, WHO-III N=5, WHO-IV N=3. Resection was complete (no residual FLAIR signal) in 9 patients, whereas 8 patients had partial resection. Adjuvant chemoradiotherapy was performed in 12 patients. Each patient was scanned up to four times: before surgery (preop), within 72 hours after surgery (postop), and at 3 and 12 months after surgery (month-3 and month-12). See Table 1 for demographic details of participants.

#	Age	Gender	Hand-edness	Present-tation	Hemi	Location	Histology (WHO grade)	Molecular signature	Lesion Vol Pre/Post (mm3)	Treat-ment
1	41	Female	Left	Seizures	Left	Frontal	Oligo (II)	*IDH* Mutated *1p19q* Lost *ATRX* Retained	166,783 94,472	Chemo-RT
2	32	Male	Right	Seizures	Right	Insula	Astro (II)	*IDH* WT *1p19q* - *ATRX* Lost	83,225 47,876	Chemo-RT
3	26	Male	Right	Seizures	Left	Temporal / Insula	GBM (IV)	*IDH* Mutated *1p19q* - *ATRX* Lost	59,000 30,153	Chemo-RT
4	49	Female	Right	Incidental	Right	Insula	Oligo (II)	*IDH* Mutated *1p19q* Lost *ATRX* Retained	31,514 37,451	Observa tion
5	55	Female	Right	Recu-rrence	Left	Frontal / SFG / frontal pole	Oligo (II)	*IDH* Mutated *1p19q* Lost *ATRX* Retained	21,098 43,358	Observa tion
6	22	Female	Left	Seizures	Right	Frontal / IFG	Ganglio-glioma (I)	*IDH* - *1p19q* - *ATRX* -	4,366 7,547	Observa tion
7	29	Male	Right	Seizures	Right	Frontal / SFG & MFG	Astro (III)	*IDH* Mutated *1p19q* Negative *ATRX* Lost	31,783 69,986	Chemo-RT
8	29	Male	Right	Seizures	Right	Frontal / MFG	Astro (III)	*IDH* Mutated *1p19q* Negative *ATRX* Lost	22,611 34,158	Chemo-RT
9	50	Male	Left	Seizures	Left	Temporal / ITG	GBM (IV)	*IDH* WT *1p19q* Negative *ATRX* Retained	15,646 15,653	Chemo-RT
10	38	Female	Right	Seizures	Right	Frontal / MFG	Oligo (II)	*IDH* Mutated *1p19q* Lost *ATRX* Retained	34,708 54,873	Chemo-RT
11	29	Male	Right	Seizures	Left	Frontal / SFG / frontal pole	Astro (II)	*IDH* Mutated *1p19q* Negative *ATRX* Lost	52,090 116,937	Observa tion
12	33	Female	Right	Head-aches	Left	Temporal / MTG	Astro (III)	*IDH* Mutated *1p19q* Negative *ATRX* Lost	87,029 84,800	Chemo-RT
13	27	Female	Right	Seizures	Left	Superior Temporal Gyrus	Ganglioglio ma (I)	*IDH* WT *1p19q* - *ATRX* -	7,592 8,533	Observa tion
14	56	Female	Right	Seizures	Left	Superior Temporal Gyrus	Astro (II)	*IDH* Mutated *1p19q* Negative *ATRX* Lost	37,392 19,188	Chemo-RT
15	32	Male	Right	Seizures	Left	Superior Temporal Gyrus	Astro (III)	*IDH* Mutated *1p19q* - *ATRX* Lost	18,035 30,280	Chemo-RT
16	27	Male	Right	Seizures	Left	SFG/SMA & Pre-central	GBM (IV)	*IDH* WT *1p19q* Negative *ATRX* Retained	73,623 43,747	Chemo-RT
17	30	Male	Right	Seizures	Left	Inferior frontal	Astro (III)	*IDH* Mutated *1p19q* - *ATRX* Lost	26,197 17,382	Chemo-RT

Table 1. Demographic and pathological information. # Number of patient, SFG, Superior Frontal Gyrus; MFG, Middle Frontal Gyrus; IFG, Inferior Frontal Gyrus; ITG, Inferior Temporal Gyrus; MTG, Middle Temporal Gyrus; SMA, Supplementary Motor Area; RT, radiotherapy; Astro – astrocytoma; GBM – glioblastoma multiforme; Oligo – oligodendroglioma; Lesion Vol Pre/Post – Total volume occupied by the tumour (Pre) and total amount of resected tissue (Post) according the lesion mask manually drawn on the MPRAGE image and refined with Unified Segmentation Lesion toolbox.

MRI and NODDI data acquisition and pre-processing

MRI data were acquired using a Siemens Magnetom Prisma-fit 3 Tesla MRI scanner and 16-channel receive-only head coil (Siemens AG, Erlangen, Germany). A T1-weighted MRI [magnetization-prepared rapid gradient-echo (MPRAGE) sequence] was acquired using the following parameters: repetition time (TR) = 2300 ms, echo time (TE) = 2.98 ms, flip angle (FA) = 9 deg, 1 mm^3 isotropic voxel resolution and a Field of View (FoV) = 256×240 mm^2, 192 contiguous slices and acquisition time of 9 minutes and 14 seconds.

During the same scanning session, we acquired a recently developed MRI multi-shell diffusion technique, Neurite Orientation Dispersion and Density Imaging (NODDI) with 30 gradient directions with b-value=800 mm/s, 60 gradient directions with b-value=2000 mm/s and ten unweighted B0 images. Other acquisition parameters were: TR = 8200 ms, TE = 95 ms, 2.5 mm^3 voxel resolution, 60 slices, FOV = 240 mm and acquisition time of 15 minutes and 19 seconds. Images were corrected for B0 field inhomogeneity, Gibbs artefacts and eddy-current distortions using MRtrix 3 (https://www.mrtrix.org/) and FSL 5.0 (http://fsl.fmrib.ox.ac.uk). All scans and processed data were visually inspected by an experienced researcher (RRG).

NODDI Matlab Toolbox (http://mig.cs.ucl.ac.uk/index.php?n=Tutorial.NODDImatlab) was used to quantify the microstructural complexity of dendrites and axons *in vivo* (Zhang et al., 2012). Compared with traditional Diffusion Tensor Imaging (DTI), the multi-compartment tissue model implemented in this toolbox disentangles two key contributing factors of Fractional Anisotropy: the Gaussian contribution from water molecules located in the extracellular space (defined as the space around neurites), and the restricted non-Gaussian diffusion that takes place in the intra-cellular space that is bounded by axonal and dendritic membranes. The apparent intra-cellular volume fraction that represents the fraction of dendrites and axons was used here as a measurement of Neurite Density.

Lesion masking and image transformation to standard space

Lesion masks were created using a semi-automated procedure. An experienced neurosurgeon (MH) initially did a manual delineation of lesion masks for each participant on the preoperative T1 image slices that included the tumour, and the resection site and damaged tissue on the follow-up T1 images. Resulting masks were refined by the Unified Segmentation with Lesion toolbox (https://github.com/CyclotronResearchCentre/USwithLesion) that uses tissue probability maps to create a posterior tumour/lesion probability map. Inter-regional distances to the tumour boundary as defined in the tumour mask were estimated as the geodesic distance of the shortest path constrained by the white matter.

For each scan, the first B0 image of the diffusion sensitive sequence was linearly coregistered to the T1 image using FSL FLIRT. The resulting inverse transformation was used to map the Neurite Density map into the T1 image space. Each T1 image was non-linearly coregistered to standard space using FSL FNIRT, but excluding the tumour/lesion mask from the non-linear step of the wrapping to avoid distorting the spatial distribution of the tumour/lesion. The resulting transformation was additionally

used to map the lesion mask and the Neurite Density map from T1 space to standard template space. The ICBM 2009a symmetric brain, an unbiased non-linear average of the MNI152, was used here as a standard template for normalisation of Neurite Density using the contralateral values hemisphere that contained the tumour.

Networks atlas and meta-analysis maps based on normative data

Functional meta-activation maps were downloaded from Neurosynth (https://neurosynth.org/), a platform for large-scale, automated synthesis of functional MRI that included data from 507,891 activation maps reported in 14,371 studies. Neurosynth generates statistical inference maps (*i.e.*, Z and p-value maps) which display the likelihood of a given term being used in a study if activation is observed at a particular voxel. We used four terms related to the four cognitive domains assessed by this study: attention, memory, perception and calculation (Figure 1, top left corner). This resulted in four meta-analysis uniformity maps that were binarised at Z=0 (*i.e.* negative values ignored).

We additionally exploited the map of large-scale networks defined in Yeo et al. (2011). This atlas was created by clustering functionally coupled regions in 1000 young, healthy adults. Analogous to meta-analytic maps derived from Neurosynth, regions delimited on the 7-Network liberal version of the Yeo atlas were used as Regions of Interest (ROIs) for calculating tumour overlap and Neurite Density (Figure 1, top right corner).

Tumour overlapping and Neurite Density estimation

As location of the tumour varied across patients, we calculated, for each ROI and participant, the "Tumour Overlap Index" as the proportion of regional volume (in mm^3) that spatially overlapped with the tumour (for preoperative assessments) or the lesion (for postoperative and follow-up assessments) according to the tumour/lesion masks, after being transformed to standard space.

Median Neurite Densities in each ROI defined on the 7-network Yeo atlas and the 4 Neurosynth maps were calculated for each participant. Only voxels of the ROI that were not overlapping with the tumour/lesion mask were included in the analysis to reduce the impact of tumour volume on Neurite Density estimation. See Figure 1 for an illustrative flowchart.

Cognitive assessment

Immediately after each MRI scanning session, cognitive performance was evaluated using the OCS-bridge tablet-based screening tool (https://ocs-bridge.com/), which is specifically designed for clinical setting. OCS-Bridge automatically compares a patient score to the distribution ('norm') for people of the same age, sex and educational history sampled from 300 healthy volunteers. We selected 10 screening tasks designed to assess 6 major cognitive domains: attention, memory, perception, praxis, language and number processing. For each individual task, a z-score value was computed by subtracting the mean and dividing by the standard deviation of task scores across participants. Tasks defined by an inverted scale where high values represent low cognitive performance were flipped by multiplying the z-score by -1. By subtracting the preoperative z-score from the z-score of each subsequent task, we defined the longitudinal trajectory of each assessment (Δ) where negative scores represent worse performance than before surgery (*i.e.* cognitive deficit) and positive scores are associated with increased performance than before surgery (*i.e.* cognitive recovery). For each of the 6 domains, score was calculated as the average z-score of all tasks associated to that domain: attention (space/object neglect and accuracy, perseveration and organisation index, sustained attention, target detection, consistency and space bias), perception (visual field, perception and extinction, visual acuity, line bisection, object perception), memory (free

verbal and episodic memory, orientation, forward and backward digit span, prospective and retrospective memory), language (picture naming, semantics, reading), praxis (hand and finger positions) and number processing (calculation and number writing).

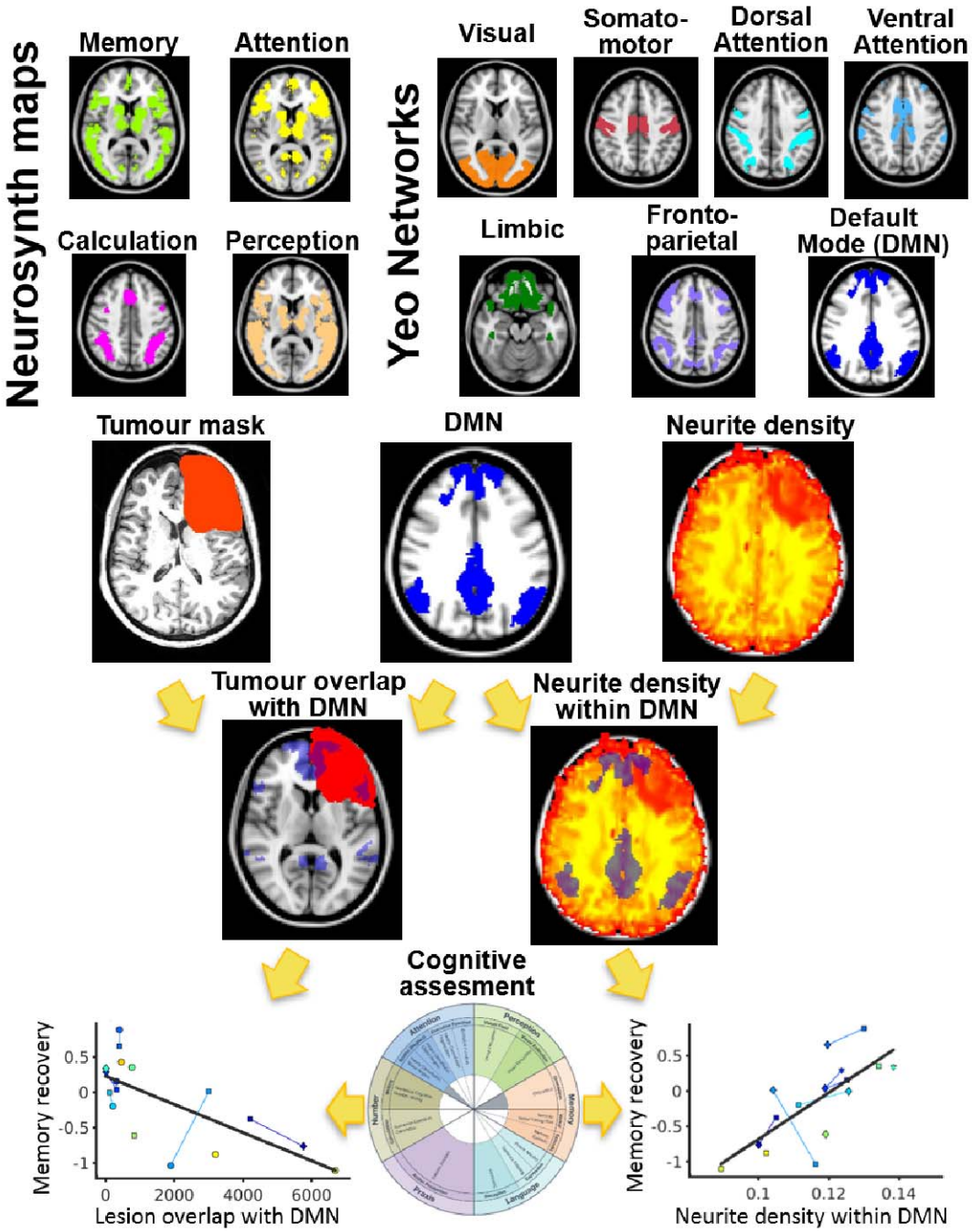

Figure 1. Flowchart of pipeline analysis. After transforming lesion masks to standard space, lesion spatial overlap and Neurite Density was calculated for each of the seven networks defined by Yeo et al. (2011) (top right) and each of the four Neurosynth meta-analysis maps considered here (attention, memory, perception and calculation; top left). For each assessment (postoperative, 3

months and 12 months), overlap and Neurite Density were compared with cognitive recovery of each domain across participants. DMN – default mode network

Statistical analysis

When the Kolmogorov-Smirnov normality test rejected the null hypothesis of data being sampled from a normal distribution, Spearman's rank was used to test associations between imaging and cognitive data. Pearson's correlation was used otherwise. Statistical tests that incorporated more than one assessment from the same patients violates the assumption of independent data. Under this scenario, we tested the association between variables using a Linear Mixed Effect Model (LMM) with random intercept and slope that incorporated total tumour volume and total neurite density (only for NODDI analyses) as covariates:

$$Cog = 1 + \beta_x \cdot X + \beta_{vol} \cdot vol + \beta_{ND} \cdot ND + (1 + X \mid subject)$$

where *Cog* represents cognitive performance of a given domain (memory, attention, perception and number processing), *X* is the predictor variable based on imaging data (*i.e.* tumour overlap or Neurite Density for a given network or Neurosynth map), *vol* is the total volume of the lesion, *ND* is the total Neurite Density of the participant (only included for predictions based on Neurite Density) and $(1 + X \mid subject)$ represents the random intercept and slope. All statistical tests were corrected for multiple comparisons using Benjamini–Hochberg False Discovery Rate (FDR < 0.05).

RESULTS

Cognitive recovery trajectories

OCS-Bridge cognitive assessment was completed by 17 patients before surgery, 8 after surgery, 7 after 3 months and 4 after 12 months. Surgical resection and treatment had an impact on cognitive performance in most participants. Attention, Perception, Memory and Number processing showed a variety of trajectories, including progressive impairment, impairment followed by recovery, no change and improvement after surgery and during recovery (**Figure 2**). Language and Praxis tests showed no sensitivity to capture deficits in our cohort except for two participants. Consequently, these two domains were not considered in further analyses. Cognitive performance was not independent across cognitive domains. Most of the four domains considered in subsequent analyses (Attention, Perception, Memory and Number processing) showed a weak positive association among each other that was significant only for Memory and Attention (R^2= 0.26, P<0.05), but that did not survive FDR correction for multiple comparisons (**Figure S1**).

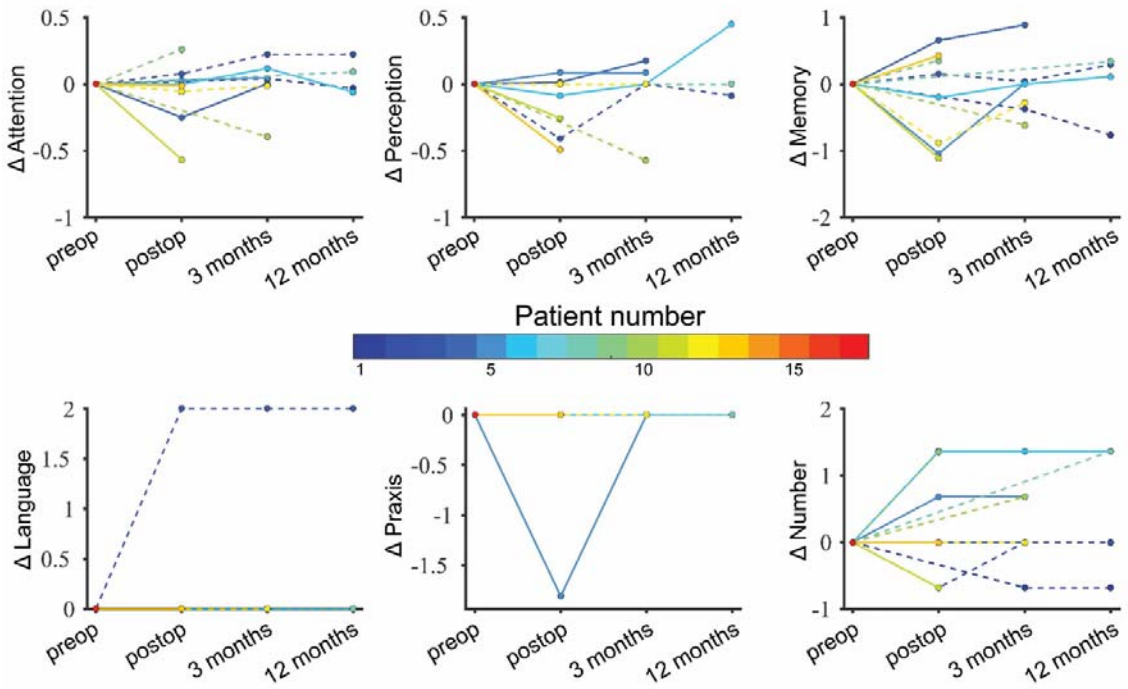

Figure 2. Cognitive performance across assessments. Mean z-scores of each participant normalised to preoperative performance in the six cognitive domains assessed by OCS-Bridge. Each colour represents an individual participant as presented in Table 1. Solid lines represent patients receiving no further treatment beyond surgery while dashed lines correspond with patients that also underwent chemo-radiotherapy. Note that lines overlap at zero for language and praxis in most patients.

Impact of tumour volume and tumour overlap on cognitive recovery

The influence of the tumour and its treatment on cognitive recovery was initially evaluated by comparing the total lesion volume with changes in cognitive performance. We found that although attention and memory deficits showed a trend of negative correlation, only number processing deficits were significantly correlated with lesion volume (ρ=-0.66, LMM, P_{fdr}<0.05, **Figure 3**).

Tumours were located on frontal (5 Left Hemisphere -LH- and 4 Right hemisphere -RH-), temporal (6 LH) and insular (2 RH) cortices (**Figure S2**). Postoperative and follow-up performance on each of the four cognitive domains assessed by OCS-bridge (attention, memory, perception, and number processing) was not significantly different in participants with frontal, temporal and insular tumours (**Figure S3;** LMM; all P>0.05). We found significant associations between attention and memory changes immediately post-surgery with tumours located on specific brain networks. Postoperative attention deficits were correlated with tumours overlapping with Ventral Attention network (ρ=-0.45, P_{fdr}<0.05) and with attention-related regions (ρ=-0.74, P_{fdr}<0.05; as defined by Neurosynth meta-analysis; **Figure 4A**). Similarly, postoperative memory deficits were significantly associated with tumours overlapping with the Dorsal Attention Network (ρ=-0.46, P_{fdr}<0.05) and DMN (ρ=-0.60, P_{fdr}<0.05). When follow-up assessments were included in the analyses (3 months and 12 months), we found a significant association between Attention deficits and tumours overlapping with DMN (ρ=-0.57, P_{fdr}<0.05) and attention-related regions (ρ=-0.53, P_{fdr}<0.05). Memory deficits were also correlated with tumours overlapping with DMN (ρ=-0.59, P_{fdr}<0.05; **Figure 4B**). All associations were tested using LMM after regressing out total lesion volume effects.

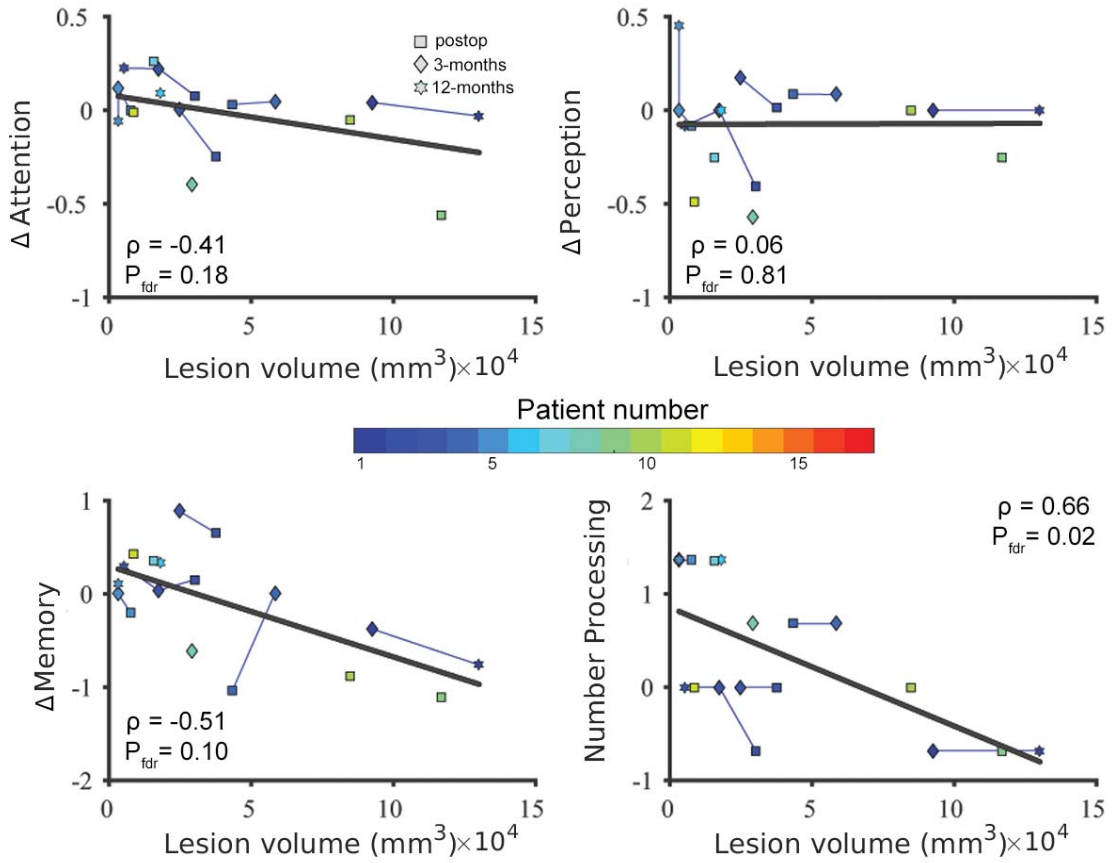

Figure 3. Association between lesion volume and cognitive recovery across patients. Cognitive recovery refers to average cognitive performance in each domain normalised to preoperative scores (positive scores correspond with post-surgical recovery and negative scores to post-surgical deficits). Colours illustrate each individual participant with lines connecting them.

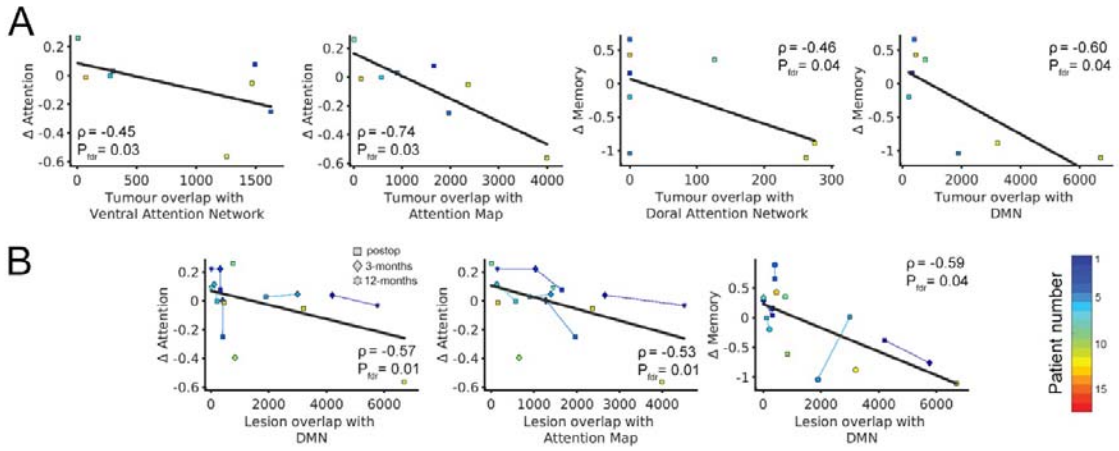

Figure 4. Cognitive deficits as a function of tumour overlapping with Yeo networks and Neurosynth maps. (a) Postoperative cognitive deficits as a function of tumour overlap with Yeo networks and Neurosynth maps. Cognitive performance was normalised to pre-surgical values and overlap values were defined as the number of voxels (equivalent to mm^3) of the tumour mask that overlapped with each network. **(b)** Cognitive deficits during recovery (postoperative, 3 months and 12 months) as a

function of lesion overlap with Yeo networks and Neurosynth maps. Lines link assessments that correspond to the same participant. None of the other domains or networks showed any significant association that survived correction for multiple comparisons.

Peri-tumoural effect of tumours on Neurite Density

The impact of tumours and their treatment on brain structure were also explored using a Neurite Density marker derived from diffusion imaging based on NODDI. We found that average Neurite Density outside the tumour was negatively associated with tumour volume (R^2= 0.28, P<0.05, **Figure S4**), suggesting that the impact of the tumour on structural integrity may not be restricted to tumoral regions alone. In support of this hypothesis, we found a distance-effect on Neurite Density as a function of distance to the tumour boundary. Peri-tumoural regions located between 0 and 20 mm from the tumour boundary had up to half of the Neurite Density compared to contralateral regions (**Figure 5**).

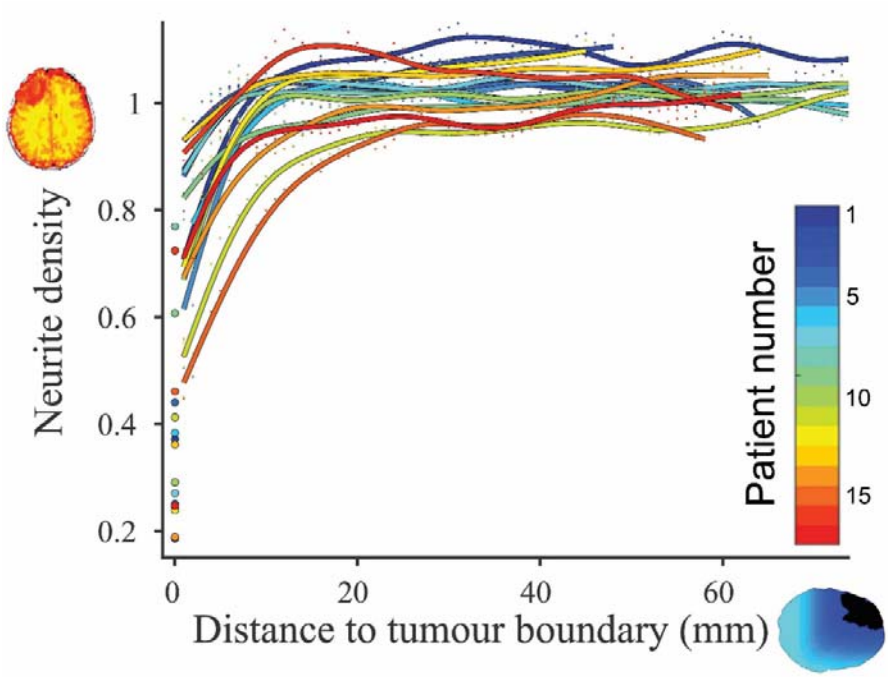

Figure 5. Neurite Density as a function of distance to the tumour boundary. Values are normalised to the contralateral hemisphere (*i.e* values less than one represent regions with reduced neurite density). Zero distance (x=0) corresponds to average Neurite Density values within each tumour. Each colour represents an individual participant.

Associations between Neurite Density within brain networks and cognitive recovery

Preoperative Neurite Density within Frontoparietal Network in both hemispheres (*i.e.* not normalised) was positively correlated with attention and memory deficits during recovery, suggesting that Neurite Density has an initial protective effect on outcome (ρ=0.30, P_{fdr}<0.05 and ρ=0.85, P_{fdr}<0.05, respectively; **Figure 6A**). Moreover, Neurite Density during recovery was also associated with cognitive deficits. When postoperative and follow-up Neurite Density values were considered, Attention and Memory deficits were correlated with Neurite Density within Ventral Attention (ρ=0.53, P_{fdr}<0.05 for attention), Frontoparietal (ρ=0.54, P_{fdr}<0.005 for attention and ρ=0.79, P_{fdr}<0.05 for memory) and DMN (ρ=-0.59, P_{fdr}<0.005 for attention and ρ =-0.84, P_{fdr}<0.05 for

memory; **Figure 6B**). All associations were tested using LMM after regressing out total lesion volume and total Neurite Density effects.

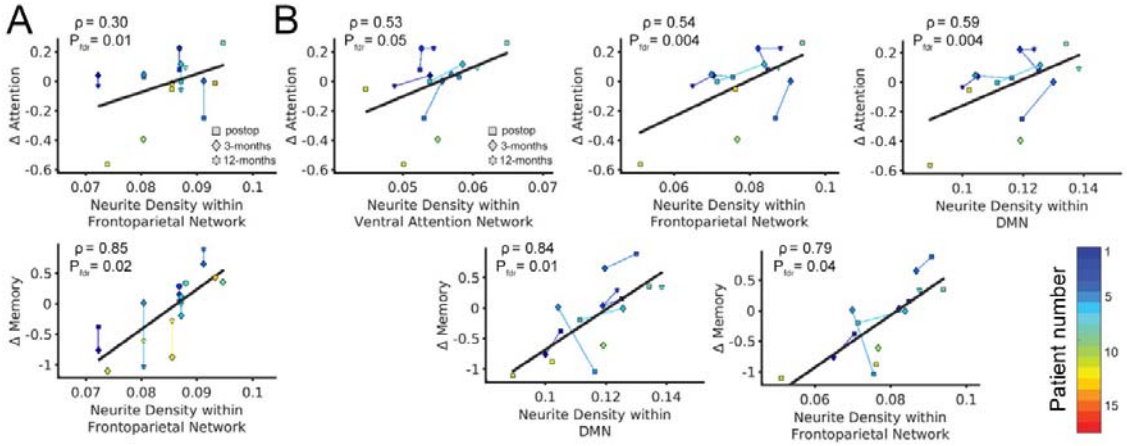

Figure 6. Cognitive deficits as a function of Neurite Density within Yeo networks and Neurosynth maps. **(a)** Cognitive deficits during recovery (postoperative, 3 months and 12 months) as a function of preoperative Neurite Density within brain networks. For a given participant, the same Neurite Density (preoperative) value was used in all assessments, resulting in vertical lines between them. **(b)** Cognitive deficits as a function of Neurite Density within brain networks during recovery (postoperative, 3 months and 12 months). Cognitive deficits are normalised to preoperative values and Neurite Density corresponds with the median density within the White Matter of each network, excluding tumour and lesion regions. None of the other domains or networks showed any significant association that survived correction for multiple comparisons. Colours illustrate each individual participant with lines connecting them.

DISCUSSION

In this study, we combined MPRAGE and NODDI diffusion MRI with normative brain network data from healthy participants and functional metanalysis maps derived from Neurosynth to determine whether cognitive trajectories are affected by the tumour in cognitive-related circuits. We found that attention and memory deficits were associated with lesion overlap with Attentional Network, DMN and attentional-related regions. Conversely, Neurite Density derived from NODDI was compromised not only at the location of the tumour, but also in the area surrounding the tumour, revealing that focal tumours can induce distant disruption in brain tissue. Here, attention and memory recovery were associated with higher Neurite Density within Frontoparietal networks (pre-operatively) and also within the DMN and attention networks (postoperatively and follow-up). Overall, these results suggest that the effect of a tumour on the brain and its cognitive consequences depends on interactions with brain networks and cognitive-related regions at both local and global levels.

Using a tablet-based cognitive assessment app afforded specific advantages, such as avoiding reliance on having a trained neuropsychologist available (with associated time and financial costs), more easily facilitating follow-up screening, and collecting specific data that is difficult to acquire using traditional clinical interviews tests, such as accurate reaction times and interactive visuospatial paradigms. In contrast to a previous paper version of this test having shown sensitivity to detect longitudinal changes in all domains under other neurological conditions (Demeyere et al., 2015; Kong et al., 2016), our OCS-Bridge assessments did not find longitudinal language and praxis changes

in this sample, presumably because deficits were too subtle and effect sizes too small at our sample size, suggesting that OCS-Bridge may be complemented by other evaluations that specifically screen these domains. For the remaining domains – attention, memory, perception and number processing – we observed a variety of cognitive recovery trajectories after surgery and during subsequent treatment that included: no cognitive change, postsurgical deterioration and then improvement, and postsurgical improvement and then deterioration. Although the mechanisms behind cognitive improvement after major surgery are not understood, previous studies have reported similar rates of cognitive recovery following tumour surgery (Habets et al., 2014; Talacchi et al., 2011). Nevertheless, given that pre- and postoperative assessments were performed in a relatively short period of time, we cannot discard the possibility of practice and learning effects on the tasks.

Tumour location is one of the most relevant features to be considered when estimating the cognitive risks of surgical resection. In our cohort, gliomas were mainly located in frontal, temporal and insular cortices on the left hemisphere. The higher prevalence of left-hemisphere tumours is because this study only included patients undergoing awake brain surgery. On the other hand, the higher prevalence of frontal, temporal and insular tumours is consistent with previous studies showing that low- and high-grade gliomas are relatively scarce in primary cortices and occipital lobes (De Witt Hamer et al., 2013; Larjavaara et al., 2007). Although several developmental, cytomyeloarchitectonic, neurochemical, metabolic, and functional reasons have been proposed, the mechanisms behind this preferential location of gliomas across the brain is still an ongoing debate (Duffau and Capelle, 2004; Ghumman et al., 2016). The presence of gliomas in secondary and association cortices that have been traditionally associated with cognitive processing (Goldman-Rakic, 1988) may be an important factor to understand cognitive deficits induced by the tumour and its treatment. Notwithstanding, we found no cognitive recovery differences between patients with frontal, temporal or insular tumours. We detected a trend of a negative association between cognitive recovery and total tumour volume that was significant only for number processing. Previous studies have reported that patients with larger tumours have higher risk of cognitive impairment before treatment (Tucha et al., 2000) and are aggravated by the clinical requirement of having more extensive surgical resections (Talacchi et al., 2011) and larger irradiation volumes and doses during radiotherapy (Klein et al., 2002).

Beyond the impact that tumour volume itself has on cognitive recovery, we hypothesised that cognitive deficits are associated with treatment-induced disruption of brain networks that have been previously identified as fundamental for cognition. In support of this hypothesis, we found significant associations between treatment-induced attention and memory deficits and lesion overlap with the DMN, Attentional Networks and attention-related regions derived from the Neurosynth meta-analysis. Functional networks were defined using normative data from healthy individuals and we did not explore functional networks from affected patients. Nevertheless, a decrease of functional connectivity within DMN in patients with brain tumours has been consistently reported in the literature. DMN functional connectivity is reduced in glioma patients when compared with controls in both the hemisphere ipsilateral (Esposito et al., 2012) and contralateral (Maesawa et al., 2015) to the tumour, which is particularly prominent for tumours located on the left side of the brain (Ghumman et al., 2016). Harris et al. (2014) reported that DMN integrity was associated with WHO tumour grade, but not with total lesion volume. Other networks such as language (Briganti et al., 2012) and motor (Otten et al., 2012) also had significantly lower functional connectivity in glioma patients. It has been hypothesised that network-specific functional disruption may mediate the treatment-induced decline in some cognitive domains such as attention (Charras et al., 2015) and executive function (D'Agata et al., 2013). However, more research is needed to better understand the role of these networks on the cognitive deterioration in brain tumour patients.

Not surprisingly, we found a consistent Neurite Density decrease within the tumour. Given that Neurite Density derived from NODDI and Fractional Anisotropy are strongly correlated (Zhang et al., 2012), our results align with previous evidence found from DTI studies showing that glioblastoma have reduced Fractional Anisotropy compared with corpus callosum, subcortical white matter (Beppu et al., 2005) and the rest of the brain (Sinha et al., 2002). Fractional anisotropy (FA) reduction in glioblastomas has been associated with decreased fibre density (Roberts et al., 2005) and reduced cell density markers derived from histopathological evaluation (Kinoshita et al., 2008) and cell proliferation markers (Beppu et al., 2005; Irie et al., 2018). This is also supported by histological studies revealing a strong positive correlation between FA and tumour cell density in the mouse (Kinoshita et al., 2008) and rat brains (Jespersen et al., 2010). Consequently, high-grade tumours show increased FA (White et al., 2011) that has been associated with low overall survival (Qu et al., 2016). However, the capability of FA as an independent prognostic parameter beside other established factors such as age and patient functional status is still unclear (Huber et al., 2016). For its part, NODDI has shown higher sensitivity for glioma grade differentiation than other diffusion sequences (Vellmer et al., 2018). Zhao et al. (2018) recently reported that NODDI in combination with patient age can predict glioma grade with a sensitivity and specificity of 92% and 89%, respectively. Despite these promising findings, the potential of NODDI as a predictor of patient cognitive recovery has not yet been explored in the literature.

We additionally found evidence in support of the hypothesis that tumours have both local and distant effects. Neurite Density was decreased not only within the tumour mask, but also beyond its boundary, being particularly disrupted in larger tumours. Thus, despite peri-tumoral regions being identified on T1 images as unaffected by the experienced neurosurgeon that delineated the mask, and by the semi-automatic segmentation procedure, these regions had decreased neurite density compared with the contralateral hemisphere. Long-distance tumour effects have been observed with regard to functional connectivity (Ghinda et al., 2018) and functional complexity (Hart et al., 2019). Disrupted white matter integrity has been reported in DTI studies that show decreased FA in peritumoural regions (Holly et al., 2017) and white matter tracts (Miller et al., 2012). Interestingly, Masjoodi et al. (2019) reported that FA, but not NODDI have been found to distinguish oedematous white matter fibres.

Extratumoural Neurite Density disruption had a differential impact on cognition depending on the affected brain network. We found that preoperative Neurite Density within the Frontoparietal network was associated with memory and attention recovery after surgery. Frontoparietal Network has a central role in cognitive control and network adaptability that is made possible by flexible, highly-connected regions (*i.e.* hubs) that shift more rapidly than other networks across a variety of task states (Cole et al., 2013). LaBar et al. (1999) hypothesized that memory and attention are subserved by neuronal networks that intersect at several Frontoparietal sites. More recently, attention and working memory are increasingly seen as overlapping constructs modulated by top-down mechanisms (Gazzaley and Nobre, 2012). Functional MRI studies have consistently reported activation in frontoparietal regions during memory and attentional tasks (Borst and Anderson, 2013; Huang et al., 2013). Hubs and the topological efficiency of the Frontoparietal Network have been associated with alerting and executive control subfunctions of attention (Markett et al., 2014) and memory (Sala-Llonch et al., 2014). Overall this suggests that high Neurite Density (pre and post-operatively) within the Frontoparietal Network is a protective factor in memory and attention recovery that is mediated by the prominent role of brain regions implicated in these cognitive domains. Moreover, when follow-up NODDI images were included in the analyses, we found a strong association with the DMN, Frontoparietal and Attention Networks. The DMN is affected by allocation of attentional and memory resources to the task-relevant region due to task demands

(Koshino et al., 2014; Mayer et al., 2010). The existing negative correlation between DMN and attentional networks have been traditionally interpreted as reflective competing functions. However, this anti-correlation exhibits substantial variability across time and is coordinated with broader dynamics involving the Frontoparietal Network (Dixon et al., 2017). From the connectomic perspective, cognitive performance of brain tumour patients has been associated with hub-related structural connectivity within the DMN and Frontoparietal Network in hemispheres contralateral to the tumour (Douw et al., 2019). By using connectomic metrics derived from both DTI and fMRI, Liu et al. (2016) achieved a 75% accuracy when predicting survival of high-grade glioma patients. However, further research is needed to better understand the mechanisms by which low- and high-grade glioma, and treatment disruption mediate cognitive decline.

Limitations

In the present work, brain networks were defined using normative data from healthy individuals (Yeo et al., 2011) and meta-analytic maps (Neurosynth). However, the mechanical and physiological disturbances induced by the tumour and the surgical intervention presumably have a major impact on the spatial pattern of brain networks. By using brain network templates and meta-analytic maps in standard space we neglected the potential spatial shift of brain functioning in our participants. Thus, our results should be interpreted as the potential of the tumour to disrupt the corresponding healthy network, not the actual tumour/lesion overlap with each participant's network.

Some patients had difficulties completing cognitive assessments due to the impact of surgery on their general condition. Consequently, missing follow-up data has the risk of attrition bias. While our application of the OCS-Bridge cognitive assessment app offered numerous advantages, most notably the possibility of reliable longitudinal assessments during follow-up, it is possible that this was with a compromise in sensitivity to detecting specific deficits, such as language or praxis. Further exploration of cognitive testing methods and paradigms is a priority for the field.

Treatment of the patients was decided solely on clinical criteria. As a consequence, 6 patients had only a surgical intervention while 11 additionally had different chemo-radiotherapy regimes. Chemo-radiotherapy has a dose-dependent effect on white matter structural integrity that has been associated with poor cognitive performance (Chapman et al., 2013; Connor et al., 2017; Deprez et al., 2012). Unfortunately, the contribution of the different treatment strategies to the observed brain disruption and cognitive decline cannot be untangled here due to the limited sample size. Finally, while all our patients had the pre-operative imaging appearances of a diffuse low-grade glioma, subsequent pathological examination revealed a range of histological diagnoses, in keeping with previous studies demonstrating the diagnostic limitations of standard MRI sequences. This variation in diagnoses may offer a further variable that impacts on cognitive outcomes.

Conclusion

Our findings highlight memory and attention deficits that are associated with tumours overlapping the DMN, the Attentional Network and Attention-related regions. Neurite Density is decreased beyond tumour boundary, whereas high values within frontoparietal, DMN and Attention networks are associated with better memory and attention recovery. Taken together, these results reveal the potential of combining brain network data and advanced MRI sequences to better understand and predict the impact of brain tumours and surgery on patients' cognitive outcomes.

Acknowledgements

We thank all patients for generous involvement in the study. We also thank to Luca Villa, Jessica Ingham, Alexa Mcdonald for their contribution to the study.

Funding

This research was supported by The Brain Tumour Charity and the Guarantors of Brain (RG91650).

Competing interests

The authors report no competing interests.

REFERENCES

Ahles, T.A., Root, J.C., Ryan, E.L., 2012. Cancer- and cancer treatment-associated cognitive change: An update on the state of the science. J. Clin. Oncol. 30, 3675–3686. https://doi.org/10.1200/JCO.2012.43.0116

Ajithkumar, T., Price, S., Horan, G., Burke, A., Jefferies, S., 2017. Prevention of radiotherapy-induced neurocognitive dysfunction in survivors of paediatric brain tumours: the potential role of modern imaging and radiotherapy techniques. Lancet Oncol. 18, e91–e100. https://doi.org/10.1016/S1470-2045(17)30030-X

Anderson, S.W., Damasio, H., Tranel, D., 1990. Neuropsychological impairments associated with lesions caused by tumor or stroke. Arch. Neurol. 47, 397–405.

Beppu, T., Inoue, T., Shibata, Y., Yamada, N., Kurose, A., Ogasawara, K., Ogawa, A., Kabasawa, H., 2005. Fractional anisotropy value by diffusion tensor magnetic resonance imaging as a predictor of cell density and proliferation activity of glioblastomas. Surg. Neurol. 63, 56–61. https://doi.org/10.1016/j.surneu.2004.02.034

Borst, J.P., Anderson, J.R., 2013. Using model-based functional MRI to locate working memory updates and declarative memory retrievals in the fronto-parietal network. Proc. Natl. Acad. Sci. U. S. A. 110, 1628–1633. https://doi.org/10.1073/pnas.1221572110

Bressler, S.L., Menon, V., 2010. Large-scale brain networks in cognition: emerging methods and principles. Trends Cogn. Sci. https://doi.org/10.1016/j.tics.2010.04.004

Briganti, C., Sestieri, C., Mattei, P.A., Esposito, R., Galzio, R.J., Tartaro, A., Romani, G.L., Caulo, M., 2012. Reorganization of functional connectivity of the language network in patients with brain gliomas. Am. J. Neuroradiol. 33, 1983–1990. https://doi.org/10.3174/ajnr.A3064

Caverzasi, E., Papinutto, N., Castellano, A., Zhu, A.H., Scifo, P., Riva, M., Bello, L., Falini, A., Bharatha, A., Henry, R.G., 2016. Neurite Orientation Dispersion and Density Imaging Color Maps to Characterize Brain Diffusion in Neurologic Disorders. J. Neuroimaging 26, 494–498. https://doi.org/10.1111/jon.12359

Chapman, C.H., Nazem-Zadeh, M., Lee, O.E., Schipper, M.J., Tsien, C.I., Lawrence, T.S., Cao, Y., 2013. Regional Variation in Brain White Matter Diffusion Index Changes following Chemoradiotherapy: A Prospective Study Using Tract-Based Spatial Statistics. PLoS One 8. https://doi.org/10.1371/journal.pone.0057768

Charras, P., Herbet, G., Deverdun, J., de Champfleur, N.M., Duffau, H., Bartolomeo, P., Bonnetblanc, F., 2015. Functional reorganization of the attentional networks in low-grade glioma patients: A longitudinal study. Cortex 63, 27–41. https://doi.org/10.1016/j.cortex.2014.08.010

Cole, M.W., Reynolds, J.R., Power, J.D., Repovs, G., Anticevic, A., Braver, T.S., 2013. Multi-task connectivity reveals flexible hubs for adaptive task control. Nat. Neurosci. 16, 1348–1355. https://doi.org/10.1038/nn.3470

Colgan, N., Siow, B., O'Callaghan, J.M., Harrison, I.F., Wells, J.A., Holmes, H.E., Ismail, O., Richardson, S., Alexander, D.C., Collins, E.C., Fisher, E.M., Johnson, R., Schwarz, A.J., Ahmed, Z., O'Neill, M.J., Murray, T.K., Zhang, H., Lythgoe, M.F., 2016. Application of neurite orientation dispersion and density imaging (NODDI) to a tau pathology model of Alzheimer's disease. Neuroimage 125, 739–744. https://doi.org/10.1016/j.neuroimage.2015.10.043

Connor, M., Karunamuni, R., McDonald, C., Seibert, T., White, N., Moiseenko, V., Bartsch, H., Farid, N., Kuperman, J., Krishnan, A., Dale, A., Hattangadi-Gluth, J.A., 2017. Regional susceptibility to dose-dependent white matter damage after brain radiotherapy. Radiother. Oncol. 123, 209–217. https://doi.org/10.1016/j.radonc.2017.04.006

D'Agata, F., Costa, T., Caroppo, P., Baudino, B., Cauda, F., Manfredi, M., Geminiani, G., Mortara, P., Pinessi, L., Castellano, G., Bisi, G., 2013. Multivariate analysis of brain metabolism reveals chemotherapy effects on prefrontal cerebellar system when related to dorsal attention network. EJNMMI Res. 3, 1–9. https://doi.org/10.1186/2191-219X-3-22

De Witt Hamer, P.C., Hendriks, E.J., Mandonnet, E., Barkhof, F., Zwinderman, A.H., Duffau, H., 2013. Resection Probability Maps for Quality Assessment of Glioma Surgery without Brain Location Bias. PLoS One 8. https://doi.org/10.1371/journal.pone.0073353

Demeyere, N., Riddoch, M.J., Slavkova, E.D., Bickerton, W.L., Humphreys, G.W., 2015. The Oxford Cognitive Screen (OCS): Validation of a stroke-specific short cognitive screening tool. Psychol. Assess. 27, 883–894. https://doi.org/10.1037/pas0000082

Deprez, S., Amant, F., Smeets, A., Peeters, R., Leemans, A., Van Hecke, W., Verhoeven, J.S., Christiaens, M.R., Vandenberghe, J., Vandenbulcke, M., Sunaert, S., 2012. Longitudinal assessment of chemotherapy-induced structural changes in cerebral white matter and its correlation with impaired cognitive functioning. J. Clin. Oncol. 30, 274–281. https://doi.org/10.1200/JCO.2011.36.8571

Dixon, M.L., Andrews-Hanna, J.R., Spreng, R.N., Irving, Z.C., Mills, C., Girn, M., Christoff, K., 2017. Interactions between the default network and dorsal attention network vary across default subsystems, time, and cognitive states. Neuroimage 147, 632–649. https://doi.org/10.1016/j.neuroimage.2016.12.073

Douw, L., Klein, M., Fagel, S.S., van den Heuvel, J., Taphoorn, M.J., Aaronson, N.K., Postma, T.J., Vandertop, W.P., Mooij, J.J., Boerman, R.H., Beute, G.N., Sluimer, J.D., Slotman, B.J., Reijneveld, J.C., Heimans, J.J., 2009. Cognitive and radiological effects of radiotherapy in patients with low-grade glioma: long-term follow-up. Lancet Neurol. 8, 810–818. https://doi.org/10.1016/S1474-4422(09)70204-2

Douw, L., Miller, J.J., Steenwijk, M.D., Stufflebeam, S.M., Gerstner, E.R., 2019. Altered structural hub connectivity and its clinical relevance in glioma. https://doi.org/10.1101/610618

Duffau, H., Capelle, L., 2004. Preferential brain locations of low-grade gliomas: Comparison with glioblastomas and review of hypothesis. Cancer 100, 2622–2626. https://doi.org/10.1002/cncr.20297

Esposito, R., Mattei, P.A., Briganti, C., Romani, G.L., Tartaro, A., Caulo, M., 2012. Modifications of

default-mode network connectivity in patients with cerebral glioma. PLoS One 7. https://doi.org/10.1371/journal.pone.0040231

Fan, G.G., Deng, Q.L., Wu, Z.H., Guo, Q.Y., 2006. Usefulness of diffusion/perfusion-weighted MRI in patients with non-enhancing supratentorial brain gliomas: A valuable tool to predict tumour grading? Br. J. Radiol. 79, 652–658. https://doi.org/10.1259/bjr/25349497

Ferroli, P., Broggi, M., Schiavolin, S., Acerbi, F., Bettamio, V., Caldiroli, D., Cusin, A., La Corte, E., Leonardi, M., Raggi, A., Schiariti, M., Visintini, S., Franzini, A., Broggi, G., 2015. Predicting functional impairment in brain tumor surgery: The Big Five and the Milan Complexity Scale. Neurosurg. Focus 39. https://doi.org/10.3171/2015.9.FOCUS15339

Gazzaley, A., Nobre, A.C., 2012. Top-down modulation: Bridging selective attention and working memory. Trends Cogn. Sci. 16, 129–135. https://doi.org/10.1016/j.tics.2011.11.014

Ghinda, D.C., Wu, J.S., Duncan, N.W., Northoff, G., 2018. How much is enough—Can resting state fMRI provide a demarcation for neurosurgical resection in glioma? Neurosci. Biobehav. Rev. 84, 245–261. https://doi.org/10.1016/j.neubiorev.2017.11.019

Ghumman, S., Fortin, D., Noel-Lamy, M., Cunnane, S.C., Whittingstall, K., 2016. Exploratory study of the effect of brain tumors on the default mode network. J. Neurooncol. 128, 437–444. https://doi.org/10.1007/s11060-016-2129-6

Goldman-Rakic, P., 1988. Topography Of Cognition: Parallel Distributed Networks In Primate Association Cortex. Annu. Rev. Neurosci. 11, 137–156. https://doi.org/10.1146/annurev.neuro.11.1.137

Habets, E.J.J., Kloet, A., Walchenbach, R., Vecht, C.J., Klein, M., Taphoorn, M.J.B., 2014. Tumour and surgery effects on cognitive functioning in high-grade glioma patients. Acta Neurochir. (Wien). 156, 1451–1459. https://doi.org/10.1007/s00701-014-2115-8

Harris, R.J., Bookheimer, S.Y., Cloughesy, T.F., Kim, H.J., Pope, W.B., Lai, A., Nghiemphu, P.L., Liau, L.M., Ellingson, B.M., 2014. Altered functional connectivity of the default mode network in diffuse gliomas measured with pseudo-resting state fMRI. J. Neurooncol. 116, 373–379. https://doi.org/10.1007/s11060-013-1304-2

Hart, M.G., Romero-Garcia, R., Price, S.J., Suckling, J., 2019. Global Effects of Focal Brain Tumors on Functional Complexity and Network Robustness: A Prospective Cohort Study. Neurosurgery 84, 1201–1213. https://doi.org/10.1093/neuros/nyy378

Holly, K.S., Barker, B.J., Murcia, D., Bennett, R., Kalakoti, P., Ledbetter, C., Gonzalez-Toledo, E., Nanda, A., Sun, H., 2017. High-grade Gliomas Exhibit Higher Peritumoral Fractional Anisotropy and Lower Mean Diffusivity than Intracranial Metastases. Front. Surg. 4, 1–10. https://doi.org/10.3389/fsurg.2017.00018

Huang, Q., Zhang, R., Hu, X., Ding, S., Qian, J., Lei, T., Cao, X., Tao, L., Qian, Z., Liu, H., 2014. Disturbed small-world networks and neurocognitive function in frontal lobe low-grade glioma patients. PLoS One 9. https://doi.org/10.1371/journal.pone.0094095

Huang, S., Seidman, L.J., Rossi, S., Ahveninen, J., 2013. Distinct cortical networks activated by auditory attention and working memory load. Neuroimage 83, 1098–1108. https://doi.org/10.1016/j.neuroimage.2013.07.074

Huber, T., Bette, S., Wiestler, B., Gempt, J., Gerhardt, J., Delbridge, C., Barz, M., Meyer, B., Zimmer, C., Kirschke, J.S., 2016. Fractional Anisotropy Correlates with Overall Survival in Glioblastoma. World Neurosurg. 95, 525–534.e1. https://doi.org/10.1016/j.wneu.2016.08.055

Hunter, R.D., 1980. WHO handbook for reporting results of cancer treatment. Int. J. Radiat. Biol. 38, 481–481. https://doi.org/10.1080/09553008014551861

Irie, R., Kamagata, K., Kerever, A., Ueda, R., Yokosawa, S., Otake, Y., Ochi, H., Yoshizawa, H., Hayashi, A., Tagawa, K., Okazawa, H., Takahashi, K., Sato, K., Hori, M., Arikawa-Hirasawa, E., Aoki, S., 2018. The relationship between neurite density measured with confocal microscopy in a cleared mouse brain and metrics obtained from diffusion tensor and diffusion kurtosis imaging. Magn. Reson. Med. Sci. 17, 138–144. https://doi.org/10.2463/mrms.mp.2017-0031

Jakola, A.S., Myrmel, K.S., Kloster, R., Torp, S.H., Lindal, S., Unsgård, G., Solheim, O., 2012. Comparison of a strategy favoring early surgical resection vs a strategy favoring watchful waiting in low-grade gliomas. JAMA 308, 1881–8. https://doi.org/10.1001/jama.2012.12807

Jespersen, S.N., Bjarkam, C.R., Nyengaard, J.R., Chakravarty, M.M., Hansen, B., Vosegaard, T., Østergaard, L., Yablonskiy, D., Nielsen, N.C., Vestergaard-Poulsen, P., 2010. Neurite density from magnetic resonance diffusion measurements at ultrahigh field: Comparison with light microscopy and electron microscopy. Neuroimage 49, 205–216. https://doi.org/10.1016/j.neuroimage.2009.08.053

Just, N., 2014. Improving tumour heterogeneity MRI assessment with histograms. Br. J. Cancer 111, 2205–2213. https://doi.org/10.1038/bjc.2014.512

Kamagata, K., Hatano, T., Okuzumi, A., Motoi, Y., Abe, O., Shimoji, K., Kamiya, K., Suzuki, M., Hori, M., Kumamaru, K.K., Hattori, N., Aoki, S., 2016. Neurite orientation dispersion and density imaging in the substantia nigra in idiopathic Parkinson disease. Eur. Radiol. 26, 2567–2577. https://doi.org/10.1007/s00330-015-4066-8

Kevin S. LaBar, Darren R. Gitelman, Todd B. Parrish, and M.-M.M., 1999. Neuroanatomic Overlap of Working Memory and Spatial Attention Networks.pdf 704, NeuroImage 10, 695–704.

Kinoshita, M., Hashimoto, N., Goto, T., Kagawa, N., Kishima, H., Izumoto, S., Tanaka, H., Fujita, N., Yoshimine, T., 2008. Fractional anisotropy and tumor cell density of the tumor core show positive correlation in diffusion tensor magnetic resonance imaging of malignant brain tumors. Neuroimage 43, 29–35. https://doi.org/10.1016/j.neuroimage.2008.06.041

Klein, M., Heimans, J.J., Aaronson, N.K., Van Der Ploeg, H.M., Grit, J., Muller, M., Postma, T.J., Mooij, J.J., Boerman, R.H., Beute, G.N., Ossenkoppele, G.J., Van Imhoff, G.W., Dekker, A.W., Jolles, J., Slotman, B.J., Struikmans, H., Taphoorn, M.J.B., 2002. Effect of radiotherapy and other treatment-related factors on mid-term to long-term cognitive sequelae in low-grade gliomas: A comparative study. Lancet 360, 1361–1368. https://doi.org/10.1016/S0140-6736(02)11398-5

Klein, M., Postma, T.J., Taphoorn, M.J.B., Aaronson, N.K., Vandertop, W.P., Muller, M., Van Der Ploeg, H.M., Heimans, J.J., 2003. The prognostic value of cognitive functioning in the survival of patients with high-grade glioma. Neurology 61, 1796–1798. https://doi.org/10.1212/01.WNL.0000098892.33018.4C

Kong, A.P.H., Lam, P.H.P., Ho, D.W.L., Lau, J.K., Humphreys, G.W., Riddoch, J., Weekes, B., 2016. The Hong Kong version of the Oxford Cognitive Screen (HK-OCS): validation study for Cantonese-speaking chronic stroke survivors. Aging, Neuropsychol. Cogn. 23, 530–548.

https://doi.org/10.1080/13825585.2015.1127321

Koshino, H., Minamoto, T., Yaoi, K., Osaka, M., Osaka, N., 2014. Coactivation of the default mode network regions and working memory network regions during task preparation. Sci. Rep. 4, 34–39. https://doi.org/10.1038/srep05954

Larjavaara, S., Mäntylä, R., Salminen, T., Haapasalo, H., Raitanen, J., Jääskeläinen, J., Auvinen, A., 2007. Incidence of gliomas by anatomic location. Neuro. Oncol. 9, 319–325. https://doi.org/10.1215/15228517-2007-016

Li, C., Wang, S., Yan, J.-L., Piper, R.J., Liu, H., Torheim, T., Kim, H., Zou, J., Boonzaier, N.R., Sinha, R., Matys, T., Markowetz, F., Price, S.J., 2018. Intratumoral Heterogeneity of Glioblastoma Infiltration Revealed by Joint Histogram Analysis of Diffusion Tensor Imaging. Neurosurgery 0, 1–11. https://doi.org/10.1093/neuros/nyy388

Liu, L., Zhang, H., Rekik, I., Chen, X., Wang, Q., Shen, D., 2016. Outcome prediction for patient with high-grade gliomas from brain functional and structural networks, in: Lecture Notes in Computer Science (Including Subseries Lecture Notes in Artificial Intelligence and Lecture Notes in Bioinformatics). pp. 26–34. https://doi.org/10.1007/978-3-319-46723-8_4

Maesawa, S., Bagarinao, E., Fujii, M., Futamura, M., Motomura, K., Watanabe, H., Mori, D., Sobue, G., Wakabayashi, T., 2015. Evaluation of resting state networks in patients with gliomas: Connectivity changes in the unaffected side and its relation to cognitive function. PLoS One 10, 1–13. https://doi.org/10.1371/journal.pone.0118072

Markett, S., Reuter, M., Montag, C., Voigt, G., Lachmann, B., Rudorf, S., Elger, C.E., Weber, B., 2014. Assessing the function of the fronto-parietal attention network: Insights from resting-state fMRI and the attentional network test. Hum. Brain Mapp. 35, 1700–1709. https://doi.org/10.1002/hbm.22285

Masjoodi, S., Hashemi, H., Oghabian, M.A., Sharifi, G., 2018. Differentiation of edematous, tumoral and normal areas of brain using diffusion tensor and neurite orientation dispersion and density imaging. J. Biomed. Phys. Eng. 8, 251–260. https://doi.org/10.31661/jbpe.v0i0.874

Mayer, J.S., Roebroeck, A., Maurer, K., Linden, D.E.J., 2010. Specialization in the default mode: Task-induced brain deactivations dissociate between visual working memory and attention. Hum. Brain Mapp. 31, 126–139. https://doi.org/10.1002/hbm.20850

Meyers, C.A., Smith, J.A., Bezjak, A., Mehta, M.P., Liebmann, J., Illidge, T., Kunkler, I., Caudrelier, J.M., Eisenberg, P.D., Meerwaldt, J., Siemers, R., Carrie, C., Gaspar, L.E., Curran, W., Phan, S.C., Miller, R.A., Renschler, M.F., 2004. Neurocognitive function and progression in patients with brain metastases treated with whole-brain radiation and motexafin gadolinium: Results of a randomized phase III trial. J. Clin. Oncol. 22, 157–165. https://doi.org/10.1200/JCO.2004.05.128

Miller, P., Coope, D., Thompson, G., Jackson, A., Herholz, K., 2012. Quantitative evaluation of white matter tract DTI parameter changes in gliomas using nonlinear registration. Neuroimage 60, 2309–2315. https://doi.org/10.1016/j.neuroimage.2012.02.033

Mohsen, L.A., Shi, V., Jena, R., Gillard, J.H., Price, S.J., 2013. Diffusion tensor invasive phenotypes can predict progression-free survival in glioblastomas. Br. J. Neurosurg. 27, 436–441. https://doi.org/10.3109/02688697.2013.771136

Otten, M.L., Mikell, C.B., Youngerman, B.E., Liston, C., Sisti, M.B., Bruce, J.N., Small, S.A., McKhann, G.M., 2012. Motor deficits correlate with resting state motor network connectivity in patients with brain tumours. Brain 135, 1017–1026. https://doi.org/10.1093/brain/aws041

Peng, S.L., Chen, C.F., Liu, H.L., Lui, C.C., Huang, Y.J., Lee, T.H., Chang, C.C., Wang, F.N., 2013. Analysis of parametric histogram from dynamic contrast-enhanced MRI: Application in evaluating brain tumor response to radiotherapy. NMR Biomed. 26, 443–450. https://doi.org/10.1002/nbm.2882

Qu, J., Qin, L., Cheng, S., Leung, K., Li, X., Li, H., Dai, J., Jiang, T., Akgoz, A., Seethamraju, R., Wang, Q., Rahman, R., Li, S., Ai, L., Jiang, T., Young, G.S., 2016. Residual low ADC and high FA at the resection margin correlate with poor chemoradiation response and overall survival in high-grade glioma patients. Eur. J. Radiol. 85, 657–664. https://doi.org/10.1016/j.ejrad.2015.12.026

Roberts, T.P.L., Liu, F., Kassner, A., Mori, S., Guha, A., 2005. Fiber density index correlates with reduced fractional anisotropy in white matter of patients with glioblastoma. Am. J. Neuroradiol. 26, 2183–2186.

Sagberg, L.M., Drewes, C., Jakola, A.S., Solheim, O., 2017. Accuracy of operating neurosurgeons' prediction of functional levels after intracranial tumor surgery. J. Neurosurg. 126, 1173–1180. https://doi.org/10.3171/2016.3.JNS152927

Sala-Llonch, R., Junqué, C., Arenaza-Urquijo, E.M., Vidal-Piñeiro, D., Valls-Pedret, C., Palacios, E.M., Domènech, S., Salvà, A., Bargalló, N., Bartrés-Faz, D., 2014. Changes in whole-brain functional networks and memory performance in aging. Neurobiol. Aging 35, 2193–2202. https://doi.org/10.1016/j.neurobiolaging.2014.04.007

Santarius, T., Bello, L., Duffau, H., 2019. Low-grade glioma, in: Kirollos, R., Helmy, A., Thomson, S., Peter, H. (Eds.), Oxford Textbook of Neurological Surgery. pp. 75–89.

Scott, J.N., Brasher, P.M.A., Sevick, R.J., Rewcastle, N.B., Forsyth, P.A., 2002. How often are nonenhancing supratentorial gliomas malignant? A population study. Neurology 59, 947–949. https://doi.org/10.1212/WNL.59.6.947

Sinha, S., Bastin, M.E., Whittle, I.R., Wardlaw, J.M., 2002. Diffusion tensor MR imaging of high-grade cerebral gliomas. Am. J. Neuroradiol. 23, 520–527.

Talacchi, A., Santini, B., Savazzi, S., Gerosa, M., 2011. Cognitive effects of tumour and surgical treatment in glioma patients. J. Neurooncol. 103, 541–549. https://doi.org/10.1007/s11060-010-0417-0

Taphoorn, M.J.B., Klein, M., 2004. Review Cognitive deficits in adult patients with brain tumours. Lancet 31, 159–168.

Tucha, O., Smely, C., Preier, M., Lange, K.W., 2000. Cogntive deficits before treatment among patients with brain tumors. Neurosurgery 47, 324–333. https://doi.org/10.1097/00006123-200008000-00011

van Dellen, E., Douw, L., Hillebrand, A., Ris-Hilgersom, I., Schoonheim, M., Baayen, J., de Witt Hamer, P., Velis, D., Klein, M., Heimans, J., Stam, C., 2012. MEG Network Differences between Low- and High-Grade Glioma Related to Epilepsy and Cognition. PLoS One.

Vellmer, S., Tonoyan, A.S., Suter, D., Pronin, I.N., Maximov, I.I., 2018. Validation of DWI pre-

processing procedures for reliable differentiation between human brain gliomas. Z. Med. Phys. 28, 14–24. https://doi.org/10.1016/j.zemedi.2017.04.005

Wang, N., Zhang, J., Cofer, G., Qi, Y., Anderson, R.J., White, L.E., Allan Johnson, G., 2019. Neurite orientation dispersion and density imaging of mouse brain microstructure. Brain Struct. Funct. 224, 1797–1813. https://doi.org/10.1007/s00429-019-01877-x

Wefel, J.S., Noll, K.R., Rao, G., Cahill, D.P., 2016. Neurocognitive function varies by IDH1 genetic mutation status in patients with malignant glioma prior to surgical resection. Neuro. Oncol. 18, 1656–1663. https://doi.org/10.1093/neuonc/now165

Wefel, J.S., Schagen, S.B., 2012. Chemotherapy-related cognitive dysfunction. Curr. Neurol. Neurosci. Rep. https://doi.org/10.1007/s11910-012-0264-9

White, M.L., Zhang, Y., Yu, F., Jaffar Kazmi, S.A., 2011. Diffusion tensor MR imaging of cerebral gliomas: Evaluating fractional anisotropy characteristics. Am. J. Neuroradiol. 32, 374–381. https://doi.org/10.3174/ajnr.A2267

Xu, H., Ding, S., Hu, X., Yang, K., Xiao, C., Zou, Y., Chen, Y., Tao, L., Liu, H., Qian, Z., 2013. Reduced efficiency of functional brain network underlying intellectual decline in patients with low-grade glioma. Neurosci. Lett. 543, 27–31. https://doi.org/10.1016/j.neulet.2013.02.062

Yeo, B.T., Krienen, F.M., Sepulcre, J., Sabuncu, M.R., Lashkari, D., Hollinshead, M., Roffman, J.L., Smoller, J.W., Zöllei, L., Polimeni, J.R., Fisch, B., Liu, H., Buckner, R.L., 2011. The organization of the human cerebral cortex estimated by intrinsic functional connectivity. J. Neurophysiol. 106, 1125–1165. https://doi.org/10.1152/jn.00338.2011

Yordanova, Y.N., Moritz-Gasser, S., Duffau, H., 2011. Awake surgery for WHO Grade II gliomas within "noneloquent" areas in the left dominant hemisphere: toward a "supratotal" resection. Clinical article. J. Neurosurg. 115, 232–9. https://doi.org/10.3171/2011.3.JNS101333

Zhang, H., Schneider, T., Wheeler-Kingshott, C.A., Alexander, D.C., 2012. NODDI: Practical in vivo neurite orientation dispersion and density imaging of the human brain. Neuroimage 61, 1000–1016. https://doi.org/10.1016/j.neuroimage.2012.03.072

Zhao, J., Li, J. bin, Wang, J. yan, Wang, Y. liang, Liu, D. wei, Li, X. bei, Song, Y. kun, Tian, Y. su, Yan, X., Li, Z. hao, He, S. fu, Huang, X. long, Jiang, L., Yang, Z. yun, Chu, J. ping, 2018. Quantitative analysis of neurite orientation dispersion and density imaging in grading gliomas and detecting IDH-1 gene mutation status. NeuroImage Clin. 19, 174–181. https://doi.org/10.1016/j.nicl.2018.04.011